THE IONOSPHERE OF SATURN: PREDICTIONS FOR PIONEER 11

J. H. Waite, Jr., S. K. Atreya, and A. F. Nagy
Space Physics Research Laboratory, Department of Atmospheric and Oceanic Science,
University of Michigan, Ann Arbor, Michigan 48109

Abstract. Model calculations indicate that the lower ionosphere of Saturn is controlled by photochemical processes, with basic features similar to the Jovian ionosphere. The scale height of the upper ionosphere is large (~3350 km). A peak electron density of $\sim 10^5 cm^{-3}$ 2250 km above a $10^{10} cm^{-3}$ reference level is expected assuming an eddy coefficient at the homopause of $1.3 \times 10^6 cm^2 s^{-1}$ and a relatively hot exosphere at 1300K.

Accepted by *Geophysical Research Letters*, July 1979

Introduction

The upcoming Pioneer 11 radio occultation observations will provide the first measurements of Saturn's ionosphere. The purpose of this paper is to present model calculations of this ionosphere, which are based on our present understanding of the controlling processes involved, as well as anticipated similarities with Jupiter. We discuss the dependence of the model results on various assumptions adopted and we show how some of these suggestions can be tested with the aid of the Pioneer 11 measurements.

Early work on the ionospheres of the major planets was reviewed by McElroy [1973]. Further quantification of the chemical and physical processes involved led to the photochemical model of the Saturn ionosphere constructed by Atreya and Donahue [1975]. Their model contained only hydrogen and helium generated ionospheric species such as H_2^+, H^+, He^+, H_3^+, and HeH^+. The model assumed a constant eddy diffusion coefficient of $2 \times 10^6 cm^2 s^{-1}$ and a cold isothermal temperature structure. Atreya and Donahue [1975] obtained a peak electron density of $10^5 cm^{-3}$ at an altitude 275 km above a reference level corresponding to $10^{16} cm^{-3}$ atmospheric density.

The work of Atreya and Donahue [1975] was extended by Capone *et al.* [1977] to include the effect of hydrocarbon ionic species as well as the contribution of galactic cosmic rays as a source of ionization. Like the earlier model of Atreya and Donahue [1975] the Capone *et al.* [1977] model assumed photochemical equilibrium for all ionospheric species, following the argument of Capone and Prasad [1973] that plasma diffusion should not affect the ionization profile. In the model they assumed a constant eddy diffusion of $2 \times 10^4 cm^2 s^{-1}$. The temperature structure was varied between an isothermal temperature of 84K and a profile due to Wallace [1975] with a stratospheric temperature inversion. Using the latter more realistic temperature structure of Wallace, they obtained a double peaked electron density profile with a maximum due to cosmic ray ionization of $7 \times 10^3 cm^{-3}$ at the $10^{19} cm^{-3}$ level and a photoionization maximum of $2 \times 10^5 cm^{-3}$ at the $10^{11} cm^{-3}$ atmospheric density level, i.e., ~1050 km above the $10^{10} cm^{-3}$ reference level.

Past models of the Saturn ionosphere have considered a limited range of values for both eddy diffusion coefficient and temperature and have not considered the effect of transport on topside ionospheric distribution. In light of recent occultation and ultraviolet measurements of Jupiter made by Pioneers 10 and 11 and Voyager 1 [Fjeldbo *et al.*, 1976; Eshleman *et al.*, 1979; Carlson and Judge, 1974; Broadfoot *et al.*, 1979] the eddy diffusion coefficient and thermal structure of the major planets may have a highly variable character. Therefore it is essential that an ionospheric model consider the impact of large variations in both the temperature and vertical mixing structure of the atmosphere. Furthermore, since the time constants associated with chemistry and diffusion of H^+ at the electron density peak are comparable it seems reasonable that both chemical and transport processes will contribute significantly to the structure of the electron density profile in the neighborhood of the peak.

Model

A large variety of spectral observations indicate that the upper atmosphere of Saturn consists of the same basic constituents as Jupiter: H_2, He, H, and CH_4. Gaseous ammonia is present only in trace quantities due to a cold trap in the lower atmosphere. Although there is some debate on the relative abundances of He [Hunten and Münch, 1973] and CH_4 [Wallace and Hunten, 1978; Sato and Hansen, 1979], for purposes of this model, values consistent with solar abundances are used. The He/H_2 ratio is taken to be 0.11 in the homosphere and the CH_4/H_2 ratio is set at 7×10^{-4}. These choices are not crucial since changes in the ratios bring about only second order changes in the ionospheric structure.

The choice of an eddy mixing profile is very important. The ionosphere may be strongly or weakly coupled to the hydrocarbon neutral atmosphere depending on whether the eddy diffusion coefficient, K, is large or small. In order to examine the range of possible cases that might arise it was necessary to construct a model which solved the coupled-continuity and momentum equations for 1) the neutral hydrocarbon species CH_4, CH_3, C_2H_2, C_2H_4, C_2H_6, and H, 2) the nonreactive neutral species H_2 and He, and 3) the flowing ionospheric species H^+. All other ionic species such as H_3^+, $C_2H_5^+$, CH_5^+, CH_4^+, CH_3^+, CH_2^+, H_2^+, HeH^+, and He^+ are maintained in photochemical equilibrium since their chemical time constants in the region of interest are much shorter than the diffusion time constant.

The reaction scheme for the neutral hydrocarbons is essentially that of Strobel [1973] using the currently available reaction rates. The ionospheric reaction scheme is similar to that of Atreya and Donahue [1976]. Table 1 lists all the ionospheric reactions included in the present model; most of these reaction rates are referenced in Atreya and Donahue [1976]. Exceptions include reactions E20 and E21 due to Capone *et al.* [1977] and the estimated recombination rate of CH_3^+ ($1.9 \times 10^{-6} cm^3 s^{-1}$). The temperature dependence of reactions R1, R4 and R5 have also been included using the dissociative recombination rate for H_3^+ of Leu *et al.* [1973] $\alpha_R = 2.8 \times 10^{-7} (200/T_e)^{0.5}$ and the radiative recombination rate for H^+ and He^+ due to Seaton [1959] of $5 \times 10^{-12} (250/T_e)^{0.7}$.

The solar fluxes used in the calculation are from Heroux and Hinteregger's F74113 compilation [Heroux and Hinteregger, 1978] and have been modified to take into account the change in the solar flux between 1974 and 1978 [H. E. Hinteregger, personal communication, 1978]. The solar flux was further modified to take into account the distance between Saturn and the Sun. A diurnal average factor of one-half and a solar zenith angle of 60° are used to bring the model in line with previous planetary ionosphere studies of rapidly rotating planets. The hydrocarbon photoabsorption cross sections are those of Mount *et al.* [1977], Mount and Moos [1978], and Watanabe *et al.* [1953]. In the case of CH_4, ionization cross sections measured by Metzger and Cook [1964] and Lukirskii *et al.* [1964] were used and branching ratios for the various processes

$$CH_4 + h\nu \rightarrow CH_4^+, CH_3^+, CH_2^+ + \text{products}$$

were taken from the results of measurements by Diebler *et al.* [1965]. For CH_3, the ionization cross section at Lyman alpha was taken to be $2 \times 10^{-17} cm^2$, consistent with Strobel's estimate [D. F. Strobel, personal communication, 1974].

The diffusion equation for all neutral species were of standard form and included both eddy and molecular diffusion. Molecular diffusion coefficients were taken from the compilation of Mason and Marrero [1970]. The diffusion equation for H^+ took the form appropriate for ambipolar diffusion in an ionosphere containing only one major ionic species [Banks and Kockarts, 1973; Bauer, 1973]. The diffusion coefficients were taken from Banks and Kockarts [1973] and included both elastic collisions with neutrals and resonance charge exchange.

Paper number 9L1102.
0094-8276/79/009L-1102$01.00

TABLE 1. Ion Chemistry

P1	$H_2 + h\nu$	$\rightarrow H_2^+ + e$
P2		$\rightarrow H^+ + H + e$
P3	$He + h\nu$	$\rightarrow He^+ + e$
P4	$H + h\nu$	$\rightarrow H^+ + e$
P5	$CH_4 + h\nu$	$\rightarrow CH_4^+ + e$
P6		$\rightarrow CH_3^+ + H + e$
P7		$\rightarrow CH_2^+ + 2H + e$
P8	$CH_3 + h\nu$	$\rightarrow CH_3^+ + e$
E1	$H_2^+ + H_2$	$\rightarrow H_3^+ + H$
E2	$H_2^+ + H$	$\rightarrow H^+ + H_2$
E3	$He^+ + H_2$	$\rightarrow H_2^+ + He$
E4		$\rightarrow HeH^+ + H$
E5		$\rightarrow H^+ + H + He$
E6	$He^+ + CH_4$	$\rightarrow CH^+ + H_2 + H + He$
E7		$\rightarrow CH_2^+ + H_2 + He$
E8		$\rightarrow CH_3^+ + H + He$
E9		$\rightarrow CH_4^+ + He$
E10	$H^+ + H_2 + H_2$	$\rightarrow H_3^+ + H_2$
E11	$H^+ + CH_4$	$\rightarrow CH_3^+ + H_2$
E12		$\rightarrow CH_4^+ + H$
E13	$HeH^+ + H_2$	$\rightarrow H_3^+ + He$
E14	$H_3^+ + CH_4$	$\rightarrow CH_5^+ + H_2$
E15	$CH^+ + H_2$	$\rightarrow CH_2^+ + H$
E16	$CH_2^+ + H_2$	$\rightarrow CH_3^+ + H$
E17	$CH_3^+ + CH_4$	$\rightarrow C_2H_5^+ + H_2$
E18	$CH_4^+ + CH_4$	$\rightarrow CH_5^+ + CH_3$
E19	$CH_4^+ + H_2$	$\rightarrow CH_5^+ + H$
E20	$CH_5^+ + CH_4 + M$	$\rightarrow C_2H_9^+ + M$
E21	$C_2H_5^+ + H_2 + M$	$\rightarrow C_2H_7^+ + M$
R1	$H_3^+ + e$	$\rightarrow H_2 + H$
R2	$H_2^+ + e$	$\rightarrow H + H$
R3	$HeH^+ + e$	$\rightarrow He + H$
R4	$H^+ + e$	$\rightarrow H + h\nu$
R5	$He^+ + e$	$\rightarrow He + h\nu$
R6	$CH_5^+ + e$	$\rightarrow CH_4 + H$
R7	$C_2H_5^+ + e$	$\rightarrow C_2H_2 + H + H_2$
R8	$CH_3^+ + e$	$\rightarrow$ products

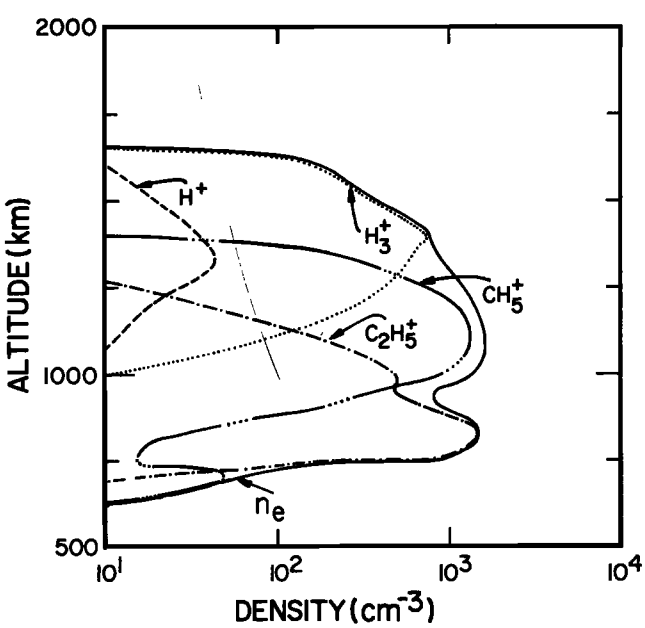

Figure 1. Ionospheric profile for Case 1. $K_h = 2.7 \times 10^9 cm^2 s^{-1}$. The temperature is isothermal at 130K. H^+ becomes the dominant ion at ~2500 km.

The lower boundary conditions on all diffusing species except for H and H^+ were fixed density conditions. For H the lower boundary condition was photochemical equilibrium. For H^+ a floating photochemical equilibrium boundary condition was chosen such that H^+ did not become numerically stiff in the calculation. The upper boundary conditions on all species but H^+ were diffusive equilibrium. For H^+ a downward flux equal in magnitude to the integrated photoproduction above the upper boundary was imposed.

Results

To isolate the effect of changing the eddy diffusion profile the temperature was held at a constant 130K and several cases with a wide range of eddy diffusion values were run. Two representative cases are shown in Figures 1 and 2. In both of the cases shown $K \propto 1/\sqrt{M}$ where M is the atmospheric density. Case 1, however, used a higher value of eddy coefficient at the reference level and as such reaches a value of $2.7 \times 10^9 cm^2 s^{-1}$ at the methane homopause whereas the value of K at the homopause in Case 2 is only $1.3 \times 10^8 cm^2 s^{-1}$. Vast differences in peak electron density and ion composition can be seen in the two cases.

In Case 1 the methane homopause was at an altitude about 1250 km above a $10^{10} cm^{-3}$ reference density level at which point the eddy diffusion has attained a value of $2.7 \times 10^9 cm^2 s^{-1}$. The atmosphere is isothermal at 130K. In this case the peak of the ionization processes were below the homopause in the altitude range 1000 to 1200 km at an atmospheric density level of $\sim 10^{10} cm^{-3}$. As a result of this, all ionization was quickly converted to hydrocarbon ions: in the case of H_2^+ by reaction E1 followed by E14; for H^+ by reactions E10 and E11 followed by E17, E18, and E19; and for He^+ reactions E6, E7, E8, E9, and subsequent reactions eventually terminating in the higher hydrocarbon ions CH_5^+ and $C_2H_5^+$. Both CH_5^+ and $C_2H_5^+$ are molecular ions and as such have rapid electron recombination rates $1.9 \times 10^{-6} cm^3 s^{-1}$. These rapid recombination rates are important 1) in maintaining a low peak electron density $\sim 1.7 \times 10^3 cm^{-3}$ and 2) bringing about a rapid decay of the ionosphere at night τ_{decay} ~310 s. The time constant for decay at higher altitudes where H_3^+ is the dominant ion is also small, τ_{decay} ~3600 s.

In Case 1 the electron density has a double peak with a maxima due to CH_5^+ at 1100 km and a maxima due to $C_2H_5^+$ at 850 km. This lower $C_2H_5^+$ maxima is due to direct ionization of CH_3 by Lyman alpha followed by reaction E17, while the upper peak results from ionization of H_2 and He and subsequent charge exchange processes discussed earlier. Although we have violated the assumption, with regard to molecular diffusion, that H^+ is the only major ion, this does not greatly alter our results since H^+ is a minor ion in this case and the H^+ that is present near the electron peak is in virtual photochemical equilibrium due to reactions with methane. At high altitudes ~2500 km, H^+ does become the dominant ion, however, at this

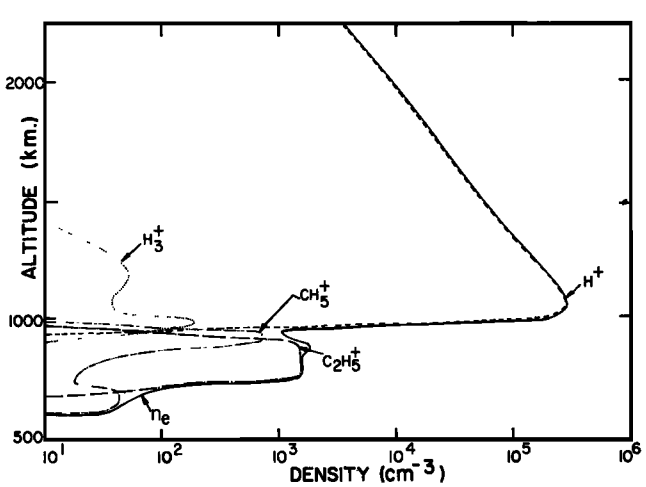

Figure 2. Ionospheric profile for Case 2. $K_h = 1.3 \times 10^8 cm^2 s^{-1}$. The temperature is isothermal at 130K.

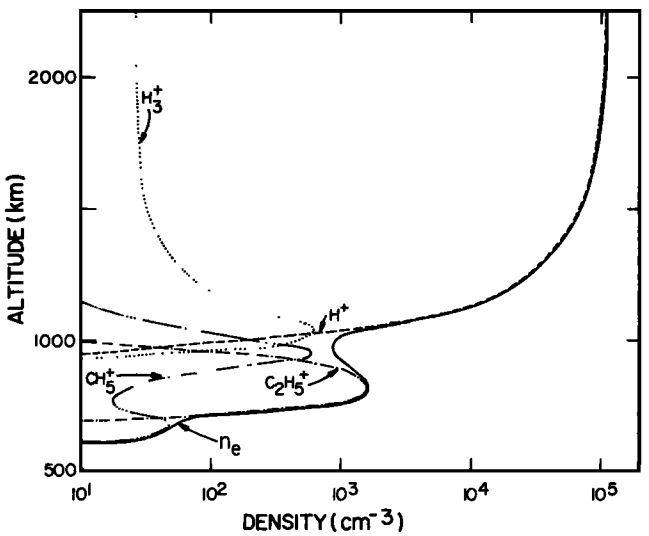

Figure 3. Ionospheric profile for Case 3. $K_h = 1.3 \times 10^6 cm^2 s^{-1}$. The temperature goes from 130K at 950 km to an exospheric temperature of 1360K at 1250 km. The peak electron density is $1.1 \times 10^5 cm^{-3}$ at an altitude of 2250 km.

altitude the density (~ 1 cm^{-3}) is undetectable by standard techniques.

In Case 2 the temperature is again isothermal (130K). However, the eddy coefficient at the homopause is greatly reduced from Case 1 ($K_h \sim 1.3 \times 10^6 cm^2 s^{-1}$). As a result the ionosphere is vastly different and much closer to previous results of [e.g., McElroy, 1973; Capone *et al.*, 1977] and the previous Jupiter model of Atreya and Donahue [1976]. In this case the methane homopause is at 800 km while the peak ionization is still occurring between 1000 and 1200 km. The dominant terminal ions in this case are much like that described by Atreya and Donahue [1976]. H^+ is the major ion at all altitudes at and above the electron density maximum. Above the peak H^+ is created by dissociative ionization (P2), direct ionization (P4), as well as reaction of H_2^+ with H (E2) and reaction of He^+ with H_2 (E5). At the peak the main loss processes are radiative recombination and downward transport to higher density regions where H^+ can undergo three body association (E10) and reactions with methane (E11, E12). These processes are responsible for the H_3^+ and CH_5^+ ions found at the base of the H^+ maxima. Again photoionization of CH_3 by Lyman alpha leads to a distinct ledge of $C_2H_5^+$ which is located at 750 km. Case 2 has a peak electron density of $2.7 \times 10^5 cm^{-3}$ at an altitude of 1100 km. The much higher peak density in this case results from the relatively slow radiative recombination and transport processes ($\tau \sim 10^6$s) which govern the loss of H^+ at the peak compared to the fast dissociative recombination processes of Case 1 ($\tau \sim 10^2$s).

The other important parameter that must be considered is the temperature. The Pioneer radio occultation observations of Jupiter [Fjeldbo *et al.*, 1976] give topside plasma temperatures > 800K. The Voyager radio occultation measurements [Eshleman *et al.*, 1979] and the ultraviolet spectrometer data [Broadfoot *et al.*, 1979] indicate temperatures to be much greater than 1000K, perhaps as large as 1500K. Two possible mechanisms which have been postulated as the source of heating are the dissipation of inertia gravity waves [French and Gierasch, 1974] and soft electron fluxes [Hunten and Dessler, 1977]. So little is known about the Saturn atmosphere at this point that it is irrelevant to go into details of possible heating sources; however, it is important to illustrate the effect of a high thermospheric temperature on the ionosphere since it appears to be a distinct possibility. To produce a reasonable temperature profile we consider a simple model with the heat sink due to IR cooling by C_2H_2 and CH_4 at an altitude slightly above the homopause and a delta function heat source approximately 300 km above the sink. Thus the equation for the temperature can be derived by using a heat conduction equation appropriate to Saturn [Atreya and Donahue, 1976; Hunten and Dessler, 1977].

Using this temperature profile (130K at 950 km and 1360K at 1250 km), with neutral gas, electron, and ion temperatures assumed equal, the ionospheric profile presented in Figure 3 was produced. Note that like Case 2, $K \propto 1/\sqrt{M}$ and reaches a value of $1.3 \times 10^6 cm^2 s^{-1}$ at the homopause. Therefore the ion chemistry is essentially the same as Case 2. All observed effects are due to the change in temperature. First there is the effect of extending the atmosphere due to a tenfold increase in scale height. This extension alters the shape of the ionosphere by increasing the H^+ scale height and by spreading out the ionization sources over a much greater altitude range. This latter effect tends to decrease the value of the electron density at the maximum. However, the inverse dependence of the recombination rates of H^+, He^+, and H_3^+ on the electron temperature partially compensates for this decrease. The result is an elongated peak density region with a maximum electron density of $1.1 \times 10^5 cm^{-3}$ between 2000 and 2500 km and a greatly extended ionosphere.

Moderate changes in the eddy diffusion profile (factors of 5) bring about only small changes in the electron density profile. For example, a factor of three increase in eddy diffusion brings about a small decrease in the electron density peak to $9.7 \times 10^4 cm^{-3}$. This decrease is the result of the deeper penetration of H^+ into the hydrocarbon layer and the resulting increase in loss rate due to downward transport of H^+. As in earlier cases, downward transport of H^+ is an important loss process at the electron peak as seen by comparing the transport time of 4.6×10^6s to the chemical loss time of 6.8×10^6s.

Discussion

The Voyager observations of the Jovian ionosphere [Eshleman *et al.*, 1979] and neutral atmosphere [Broadfoot *et al.*, 1979] tend to support an atmosphere with relatively high exospheric temperature and modestly low eddy mixing coefficient. One expects the Saturn atmosphere to manifest similar physicochemical characteristics as Jupiter. Therefore, our model calculations corresponding to $T_{ex} =$ 1360K and $K_h = 1.3 \times 10^6 cm^2 s^{-1}$ are likely to be representative of the conditions at the time of Pioneer 11 encounter with Saturn. One should however keep in mind that the Pioneer and Voyager observations of Jupiter provide only two data sets, one at solar minimum and the other at solar maximum. It is not certain that the variation between these two sets implies a corresponding solar cycle variation. We have therefore also presented cases with a relatively high K_h value of $2 \times 10^9 cm^2 s^{-1}$. It is interesting to note that if K_h were indeed as large as $2 \times 10^9 cm^2 s^{-1}$, one would expect the photochemically driven ionosphere to almost entirely disappear at night since the time constant for the removal of the dominant ions (H_3^+, $C_2H_5^+$, and CH_5^+) is on the order of one hour. No major diurnal change in the electron density is expected if the major ion in the upper ionosphere is H^+ and the exospheric temperature is <1000K as is the case with low

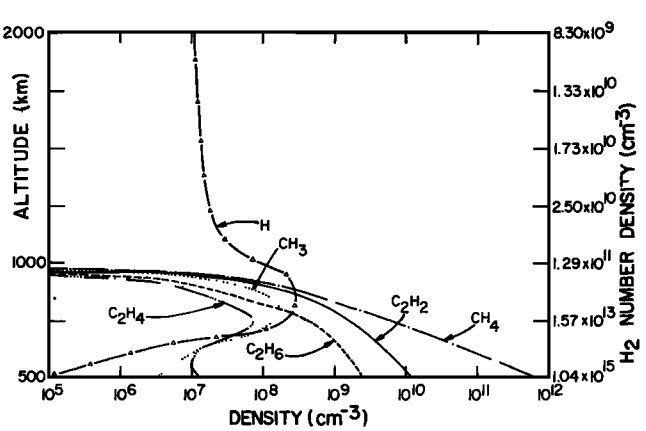

Figure 4. The neutral atmosphere for the nominal case, Case 3. The H_2 number densities corresponding to the altitudes (left ordinate) are shown on the right ordinate. Above 850 km the atmospheric density is equivalent to the H_2 density.

K_h (Case 2). However, if the exospheric temperature is much greater than 1000K significant decay of the daytime ionosphere may occur during the night [Atreya *et al.*, 1979].

In addition to the photochemical production of ions, there is a possibility of long-lived metallic ions as had been predicted [Atreya *et al.*, 1974] and their evidence was detected at Jupiter both by Pioneer and Voyager spacecrafts. Such ions could be a result of an electromagnetic coupling between the satellites and parent planet or could be of meteoritic origin. The planetary dynamo theory predicts a modestly large magnetic field for Saturn, although no definite measurements have yet been carried out. In the presence of a magnetic field, ion-atom interchange between Titan and Saturn is likely, although the electromagnetic coupling will be relatively weak compared to Io-Jupiter coupling due to the remoteness of Titan from Saturn. Metallic ions of meteoritic origin or cosmic ray ionization [Capone *et al.*, 1977] could still result in sporadic E-type layers in the deep ionosphere. A combination of upward propagating inertia gravity waves and magnetospheric processes (e.g., soft electron precipitation) is expected to give rise to a high exospheric temperature on Saturn. In the present calculations, we have not considered lack of equilibrium between the plasma and neutral temperatures, since such sophistication will be justified only after the first ionospheric measurements of Saturn are carried out. Plasma temperature calculations are now in progress and will be available after the encounter.

In summary, the overall characteristics of the Saturn ionosphere are not expected to differ drastically from those of Jupiter; however, planetary observations have been full of surprises.

Acknowledgments. This research was supported in part by NASA Grants NSG-7404 and NGR23-005-015 and the NSF Atmospheric Sciences Section. Acknowledgment is also made to the National Center for Atmospheric Research, which is sponsored by the National Science Foundation, for the computing time used in this research.

One of us (AFN) wishes to express his special thanks to E. G. Fontheim, who assumed the role of Editor for this paper.

References

Atreya, S. K., and T. M. Donahue, Ionospheric models of Saturn, Uranus, and Neptune, *Icarus, 24,* 358, 1975.

Atreya, S. K., and T. M. Donahue, Model ionospheres of Jupiter, in *Jupiter,* edited by T. Gehrels, University of Arizona Press, Tucson, Arizona, 1976.

Atreya, S. K., T. M. Donahue, and M. B. McElroy, Jupiter's ionosphere: Prospects for Pioneer 10, *Science, 184,* 154, 1974.

Atreya, S. K., T. M. Donahue, and J. H. Waite, Jr., An interpretation of the Voyager measurement of Jovian electron density profiles, *Nature,* in press, 1979.

Bauer, S. J., *Physics of Planetary Ionospheres,* New York: Springer-Verlag, 1973.

Banks, P. M., and G. Kockarts, *Aeronomy,* New York and London, Academic Press, 1973.

Broadfoot, A. L., M. J. S. Belton, P. Z. Takacs, B. R. Sandel, D. E. Shemansky, J. B. Holberg, J. M. Ajello, S. K. Atreya, T. M. Donahue, H. W. Moos, J. L. Bertaux, J. E. Blamont, D. F. Strobel, J. C. McConnell, A. Dalgarno, R. Goody, and M. B. McElroy, Extreme ultraviolet observations from Voyager 1 encounter with Jupiter, *Science, 204,* 979, 1979.

Capone, L. A., and S. S. Prasad, Jovian ionospheric models, *Icarus, 20,* 200, 1973.

Capone, L. A., R. C. Whitten, S. S. Prasad, and J. Dubach, The ionospheres of Saturn, Uranus, and Neptune, *Astrophys. J., 215,* 977, 1977.

Carlson, R. W., and D. L. Judge, Pioneer 10 ultraviolet photometer observations at Jupiter encounter, *J. Geophys. Res., 79,* 3623, 1974.

Diebler, V. H., M. Krauss, R. M. Reese, and F. N. Harlee, Mass-spectrometric study of photoionization. III Methane and methane-d_4, *J. Chem. Phys. 42,* 3791, 1965.

Eshleman, V. R., G. L. Tyler, G. E. Wood, G. F. Lindal, J. D. Anderson, G. S. Levy, and T. A Croft, Radio science with Voyager 1 at Jupiter: Preliminary profiles of the atmosphere and ionosphere, *Science, 204,* 976, 1979.

Fjeldbo, G., A. Kliore, B. Seidel, D. Sweetnam, and P. Woiceshyn, The Pioneer 11 radio occultation measurements of the Jovian ionosphere, in *Jupiter,* edited by T. Gehrels, University of Arizona Press, Tucson, Arizona, 1976.

French, G. R., and P. J. Gierasch, Waves in the Jovian upper atmosphere, *J. Atmos. Sci., 31,* 1707, 1974 .

Heroux, L., and H. E. Hinteregger, Aeronomical reference spectrum for solar UV below 2000Å, *J. Geophys. Res., 83,* 5305, 1978.

Hunten, D. M., and A. J. Dessler, Soft electrons as a possible heat source for Jupiter's thermosphere, *Planet. Space Sci., 25,* 817, 1977.

Hunten, D. M., and G. Münch, The helium abundance on Jupiter, *Space Sci. Rev., 14,* 433, 1973.

Leu, M. T., M. A. Biondi, and R. Johnsen, Measurements of the recombination of electrons with H_3^+ and H_5^+ ions, *Phys. Rev. A, 8,* 413, 1973.

Lukirskii, A. P., I. A. Brytov, and T. M. Yimkina, Photoionization absorption of He, Kr, Xe, CH_4, and methylal in the 23.6–250Å region, *Opt. Spctrosc. USSR English Translation, 17,* 234, 1964.

Mason, E. A., and T. R. Marrero, The diffusion of atoms and molecules, *Adv. At. Mol. Phys., 6,* 156, 1970.

Metzger, P. H., and G. R. Cook, On the continuous absorption, photoionization, and fluorescence of H_2O, NH_3, CH_4, C_2H_4, and C_2H_6 in the 600–1000Å region, *J. Chem. Phys., 41,* 642, 1964.

McElroy, M. B., The ionospheres of the major planets, *Space Sci. Rev., 14,* 460, 1973.

Mount, G. H., and H. W. Moos, Photoabsorption cross sections of methane and ethane, *Astrophys. J., 224,* L35, 1978.

Mount, G. H., E. S. Warden, and H. W. Moos, Photoabsorption cross sections of methane from 1400–1850Å, *Astrophys. J., 214,* L47, 1977.

Sato, M., and J. E. Hansen, Jupiter's atmospheric composition and cloud structure deduced from absorption bands in reflected sunlight, *J. Atmos. Sci.,* in press, 1979.

Seaton, M. J., Radiative recombination of hydrogenic ions, *Mon. Notices Roy. Astronom. Soc., 119,* 81, 1959.

Strobel, D. F., The photochemistry of hydrocarbons in the Jovian atmosphere, *J. Atmos. Sci., 30,* 489, 1973.

Wallace, L., On the thermal structure of Uranus, *Icarus, 25,* 538, 1975.

Wallace, L., and D. M. Hunten, The Jovian spectrum in the region 0.4–1.1 μm: The C/H ratio, *Rev. Geophys. Space Res., 16,* 289, 1978.

Watanabe, K., M. Zelikoff, and E. C. Y. Lin, Absorption coefficients of several atmospheric gases, Tech. Rep. 53–23, 79 pp., Air Force Cambridge Res. Lab., Bedford, Mass., 1953.

(Received June 26, 1979;
accepted July 24, 1979.)